International Journal of Multiphase Flow 36 (2010) 153–165

Contents lists available at ScienceDirect

International Journal of Multiphase Flow

journal homepage: www.elsevier.com/locate/ijmulflow

Review

Towards understanding the critical heat flux for industrial applications

Wael H. Ahmed [a,*,1], Meamer A. El-Nakla [a,1], Basel I. Ismail [b]

[a] Department of Mechanical Engineering, King Fahd University of Petroleum and Minerals, KFUPM, P.O. Box 874, Dhahran 31261, Saudi Arabia
[b] Department of Mechanical Engineering, Lakehead University, Thunder Bay, Ont., Canada P7B 5E1

ARTICLE INFO

Article history:
Received 25 May 2009
Received in revised form 8 September 2009
Accepted 15 October 2009
Available online 27 October 2009

Keywords:
Critical heat flux
Transient CHF
Burnout
Boiling crisis
CANDU systems
Nuclear applications

ABSTRACT

Understanding CHF is of an upmost importance in many industries, especially in the design and operation of boilers, nuclear power plants, cryogenic systems, etc. Due to safety issues related to the nuclear power plants, and the adaptation of CHF as the limiting criterion of power generation, it is important to understand the mechanisms of CHF relevant to nuclear systems operation. Moreover, CHF is expected to occur during transients than steady-state conditions. Therefore, knowledge of transient CHF is of great importance for the safety evaluation of nuclear reactors under transient condition. In this paper, the existing CHF experimental and modeling studies are discussed in order to understand the phenomena leading to CHF. Also, the effect of transient conditions on CHF for nuclear fuels has been evaluated.

1. Introduction

Critical heat flux (CHF) is one of the most essential quantities that forms a very important restriction in the safe operation of nuclear power reactors, such as water-cooled CANadian Deuterium Uranium (CANDU) power reactor. CHF represents the maximum heat flux a wetted surface can achieve. Any further increase in heat flux beyond the CHF will result in a sharp decrease in the heat transfer rate from the heating surface to cooling fluid. CHF can occur for a heated surface in both non-flowing (pool boiling) and flowing (forced or free convection) conditions which, for the latter case, is encountered more frequently in the cooling of nuclear power reactor components and steam generators. The mechanisms that occur in pool boiling, such as bubble nucleation, bubble growth and departure and/or collapse occur also in two-phase forced convective boiling. However, pool boiling heat transfer is relatively less complicated to characterize because the forced convection effect does not play a role, and knowledge obtained with respect to pool boiling are considered to be valuable towards understanding forced-flow boiling.

CHF occurrence can be identified when the heated surface is not in contact with the cooling liquid. Taking as reference a heat-flux controlled vertical heated pipe, two kinds of regimes are possible, depending on the dryout quality and heat flux. At low heat flux CHF occurs when the liquid film (annular flow regime) at the wall becomes depleted due to thinning. Beyond the CHF point the dispersed flow film boiling region is entered. In this situation, the occurrence of CHF is said to be due to dryout. At higher heat flux, the crisis is reached directly from nucleate boiling conditions: a vapor layer is formed separating the continuous liquid core from the heated wall. This type of flow regime is called the inverted annular film boiling regime which is characterized by more sever increase in the heated surface wall temperature which might result in physical burnout. CHF occurrence in this case is called "departure from nucleate boiling" or simply DNB.

Although, there have been several hundreds of papers published to investigate critical heat flux (CHF) behaviors and predictions at steady-state conditions for the thermalhydraulic analysis of the nuclear reactors. However, CHF is expected to occur during transients than steady-state conditions. Therefore, knowledge of transient CHF is of great importance for the safety evaluation of nuclear reactors under transient conditions.

The general approach in predicting transient CHF in nuclear reactor safety is to treat it as a local-condition phenomenon. With this approach, the steady-state correlations, coupled with instantaneous local flow conditions, are used to predict the transient CHF values. The use of steady-state correlations to predict transient CHF brings up two major concerns which are: (i) whether steady-state CHF data, or any analytical model which is derived from these data, can be applied to predict CHF onset in transient and (ii) on the basis of what parameters (e.g. local and instantaneous values of flow) CHF should be calculated in transients. The answer to the first concern is so far given in many places in the literature that CHF can be calculated from steady-state data or correlations

* Corresponding author. Tel.: +966 (3) 860 7507; fax: +966 (3) 860 2949.
E-mail address: ahmedw@kfupm.edu.sa (W.H. Ahmed).
[1] Former Research Scientists at Atomic Energy of Canada Ltd., Ont., Canada.

0301-9322/$ - see front matter © 2009 Elsevier Ltd. All rights reserved.
doi:10.1016/j.ijmultiphaseflow.2009.10.002

especially for flow reduction and power excursion accidents. However, there are no specific criteria currently available to answer the second concern.

1.1. CHF relation to the safety of nuclear reactors

Nuclear reactors are operated below the CHF. However a part of the fuel bundle can experience dryout during a loss of coolant accident (LOCA) occurrence. Dryout can also be encountered during a loss-of-regulation accident (LORA) when the reactor power accidentally increases. In the event of a large break LOCA in nuclear reactor, such as that resulting from a rupture of a pipe of a primary coolant transport system, pool boiling heat transfer considerations would play a significant role. For example, during large breaks LOCA, a significant decompression in the coolant transport system could occur that consequently could cause flow reversal in the downstream core pass. As a result, the net flow inertia within at least some fuel channels in the reactor core system goes to zero causing the coolant flow to stagnate in the fuel channels for some period of time. This condition tends to cause rapid heat-up of the pressure tubes in the fuel channels of the reactor core that might result in possible expansion of the hot pressure tubes to contact the calandria tubes, a phenomenon known as "pressure-tube ballooning", such that pool boiling becomes applicable to the nearly stagnant moderator water outside of the fuel channels in the calandria vessel (Griffith et al., 1977; NSSD, 1981). There, pool boiling dynamics such as nucleation of vapor bubbles, bubble growth and departure and/or collapse which had been absent under reactor normal operating conditions would become vigorous in such a situation, so that it would become essential to take into account these effects in the safety analysis with respect to design and operation of nuclear reactors.

For the other accident scenario, LORA, the power might accidently increase to a level that exceeds that corresponding to the CHF at normal flow conditions of pressure and flow. In this case the flow regime could change for the fuel bundle (or a part of it) from nucleate boiling to inverted annular film boiling passing through the CHF point, which is in this case DNB.

Of the three boiling heat transfer regimes; namely, nucleate, transition and film boiling, nucleate boiling is the regime most efficient and simultaneously most complex mode of boiling. By definition, nucleate boiling heat transfer is characterized by the formation of vapor bubbles from fixed sites randomly distributed on a heated surface. The boiling crisis, or burnout, phenomenon could occur in boiling-water-cooled fuel channels in the reactor core where there is a depletion of liquid film, which under normal operation flows over the fuel rods in the fuel channels, and a stable vapor film is formed over the fuel rods. Also, it could occur at reactor high powers where the rate of bubble nucleation exceeds the ability to replenish the liquid supply to the heating surface of the fuel rods. Consequently, the efficient process of nucleate boiling heat transfer suddenly deteriorates in burnout condition, whereas it gradually deteriorates in dryout condition, thus causing cooling failure and the fuel sheath (cladding) experiences a sharp rise in temperature, may be some orders of magnitude, which is a crucial characteristic of burnout behavior. This phenomenon could limit the fuel performance, and most likely cause failure in form of damaging or melting the fuel rods, which eventually result in an unsafe operation of the nuclear power reactor.

In the present paper, the review of the available literature on the steady-state and transient CHF, in order to better understand CHF phenomena, is presented. In addition, the parameters associated with the onset of CHF influenced by the transients are discussed. Also, the applicable range of flow conditions for which the steady-state correlations or prediction methods could safely be applied to effectively predict the transient CHF values is finally evaluated.

2. Theories for explaining the transient CHF

There are some theories for explaining the transient CHF phenomena such as the dryout of a thin liquid sub-layer under a vapor colt (e.g. the model of Lee and Mudawaar, 1988) or the existence of a bubbly layer between the heated surface and the liquid core (e.g. the model of Weisman and Pei (1983)). Weisman (1995) tried to explain the relation between steady-state and transient CHF phenomenologically based on studies conducted by Iwamura et al. (1994a,b) which showed that the Weisman and Pei (1983) steady-state CHF model was the best model to predict and explain the transient CHF. The Weisman–Pei steady-state CHF model assumes CHF occurs when the vapor volume fraction in the bubbly layer exceeds a critical value. The vapor content of the bubbly layer is determined by a balance between the outward flow of vapor and inward turbulent transport of liquid at the bubbly layer–core interface.

Chang et al. (1989) proposed a method of classifying the transient CHF mechanisms. The method is based on a novel transient CHF map that considered upstream and local effects. The proposed transient CHF regime map is shown in Fig. 1, and is divided into four regions:

(a) Hydraulic-Instability-Limited DNB (Regime I);
(b) Thermally-Limited DNB (Regimes II and III);
(c) Liquid-Film-Limited Dryout (Regime IV).

For each regime the CHF mechanism and transient effect are given in Table 1.

The transient CHF correction factors here were derived for each CHF regime using the local-micro-layer-depletion factor and the upstream-effect factor. The transient-correction factor K_{TR} is defined as (Chang et al., 1989)

$$K_{TR} = \frac{q_{CHF,TR}}{q_{CHF,SS}} \tag{1}$$

where $q_{CHF,SS}$ is the steady-state CHF and $q_{CHF,TR}$ is the transient CHF for the same local condition. Chang et al. (1989) proposed the transient-correction factor to have two components:

$$K_{TR} = K_{TR,m} \times K_{TR,u} \tag{2}$$

where $K_{TR,m}$ is the local transient-effect factor (micro-layer-depletion factor), and $K_{TR,u}$ is the flow-history-effect (upstream-effect fac-

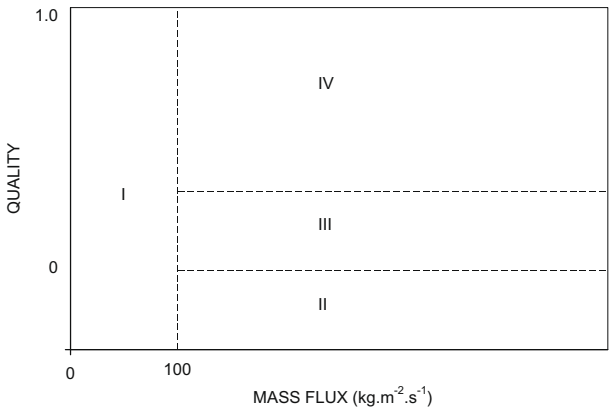

Fig. 1. Chang et al. (1989) transient CHF map.

Table 1
Transient CHF mechanism as proposed by Chang et al. (1989).

Regime		Dryout mechanism	Transient
I	Pool boiling and low flow	Hydrodynamic Instability	Micro-layer depletion
II	Sub-cooled DNB	Bubble crowding (local)	Micro-layer depletion
III	Low quality DNB and transient	Bubble crowding (bubbly layer)	Micro-layer depletion and upstream effect
IV	Annular dryout	Liquid film dryout	Upstream effect

tor). The transient-correction factor in each regime was defined (Chang et al., 1989) as follows:

$$K_{TR} = K_{TR,m} \quad \text{for regime I}$$
$$K_{TR} = K_{TR,m} \quad \text{for regime II}$$
$$K_{TR} = K_{TR,m} \times K_{TR,u} \quad \text{for regime III}$$
$$K_{TR} = K_{TR,u} \quad \text{for regime IV}$$

3. Experimental studies on CHF

The technical significance of CHF phenomenon that relates to burnout has led to the development of a variety of empirical or semi-empirical correlations and models. Many different correlations based on experimental measurements for the prediction of CHF exist in the literature and vast amount of experimental data are currently available. In general, CHF correlations are applicable to specific geometries and valid over relatively limited ranges and cannot be extended to conditions beyond the database. CHF has been measured extensively in simple flow geometries such as plates, strips, wires, and single tubes, made of various materials that have been investigated over a wide range of boiling conditions as reported in Pioro et al. (2004).

Other simple flow geometries have been used frequently in CHF experiments. Such measurements have helped to provide a better understanding of CHF behavior. One of the main problems for investigating CHF in rod bundles is very high cost of such experiments, and investigators are still attempting to find the reliable and relatively inexpensive simple flow geometry test sections to model CHF mechanisms in fuel bundles. Browne and Bansal (1999) reviewed many experimental and modeling studies on boiling over single horizontal tubes and on horizontal tube bundles with different surface geometries. CHF experiment in fuel bundles using water as a working fluid is very costly because of high pressure and temperature of water requirements in heat transport loops under standard nuclear reactor operating conditions (Ahmad, 1973; Chen et al., 2004). Therefore, in order, to reduce the high electrical power cost, parameter scaling has been attempted. One method is to scale down the size of test sections, while using the same working coolant, i.e. water. This method of scaling has been successful for simple geometries, but there is evidence that it would not work effectively for multi-rod bundles (Chen et al., 2004).

An alternative method, which has been widely used, is to replace water by a modeling fluid having a lower latent heat of vaporization, such as refrigerants for simulating CHF for water. This tends to reduce the test section power considerably. Also, the required identical liquid/vapor density ratio for both water and an environmentally safe refrigerant, such as R-134a results in much lower operating pressures and temperatures for R-134a. For example, Pioro et al. (2000) reported that reliable CHF predictions for water can be made based on CHF measurements in refrigerants at considerably lower pressures (e.g. 1.13–1.67 MPa in R-134a compared to 7–10 MPa in water), temperatures (e.g. 44–60 °C in R-134a compared to 286–311 °C in water) and powers (e.g. 0.95 MW in R-134a compared to 10 MW in water for the experiments with bundles). Consequently, scaling using refrigerants for water in CHF experiments dramatically reduces loop construction costs and allows improved visualization capability due to lower operating pressures and temperatures (Ahmad, 1973). The existing methods for the development of scaling criteria for two-phase flow systems that, for example, could simulate heat transport loops in nuclear reactor systems have been reviewed by Ishii and Jones (1976). Those methods were used by Ishii and Kataoka (1983) to develop scaling criteria for a thermalhydraulic loop, and extended by Kocamustafaogullari and Ishii (1986) for reduced-pressure and fluid-to-fluid scaling. Cheng et al. (1993) reported a range of experimental data of thermophysical properties of various modeling fluids, including R-134a, based on a series of CHF experiments that were performed to validate CHF fluid-to-fluid modeling techniques.

Early research studies, such as the work by Palen et al. (1972), have characterized boiling outside large-scale horizontal multi-tube bundles. In these studies, tube-bundle average heat transfer coefficients were obtained, and found to be greater than those for a single tube in saturated pool boiling. Hsieh et al. (2003a,b) performed an experimental study to investigate nucleate pool boiling heat transfer from plasma coated tube bundles immersed in saturated R-134a. They studied the influence of various parameters, for instance, bundle arrangements and heat flux on nucleate boiling characteristics. They observed that at low heat fluxes, the vertical-in-line tube bundles had the highest bundle factor. Other nucleate boiling studies using multi-tube bundles include investigations by Chan and Shoukri (1987), Cornwell (1990), Memory et al. (1995a,b), and Hsieh and Yang (2001). Although, there have been several studies that investigated general pool boiling characteristics on horizontal single tubes and multi-tube bundles made of different materials and operating under various boiling conditions (Hsieh and Hsu, 1994; Memory et al., 1995a,b; Chiou and Lu, 1997; Saidi et al., 1999; Hsieh and Ke, 2002; Hsieh et al., 2003a,b; Barthau and Hahne, 2004), the CHF mechanism and its relation to dynamics of dry patches formation and spreading on such geometries in sub-cooled and saturated pool boiling were not comprehensively investigated previously.

Dry patches, known also as dry areas or dry spots, on the heating surface during nucleate boiling have been reported in a number of experimental results. The occurrence of dry patches seems to indicate that the heating surface is partly in contact with the liquid. The effect of dry patches on the heating surface is very important, because the dry patches have much poorer heat transfer mechanism. In an early study by Kirby and Westwater (1965), the liquid–vapor interactions very close to the heating surface were investigated. From their results, an important consequence is that sizable dry patches may develop under the large vapor masses, whereas only small dry patches, if any, can develop under primary bubbles which are small compared to vapor masses. Kirby and Westwater (1965) concluded that the rapid growth of the dry patches seems to be responsible for the occurrence of the CHF. Van Ouwerkerk (1972) experimentally investigated the occurrence of dry patches using Pyrex or fused quartz with a conductive layer of gold having a thickness of 10 nm. When the heat flux is sufficiently high, suddenly at some point on the heating surface a dry area is not wetted and starts growing, leading to boiling crisis or burnout.

Unal et al. (1992) reported that research in the area of hot spot or dry patch CHF has involved work in three main categories: (1) thin horizontal boiling surfaces – size, formation, and growth of dry patches investigated but no work done on the contact temperature; (2) thick horizontal boiling surfaces – formation of dry patches observed; and (3) wires – spatial distribution of dry

patches along the length of a wire, with much "CHF hot spot temperature" work done. Dry patch formation on horizontal flat boiling surfaces and horizontal wires could show slightly different characteristics because of the hydrodynamics of the vapor mushrooms. In the work done by Unal et al. (1992), emphasis was given to the formation of dry patches on horizontal flat boiling surfaces. In their model, they hypothesized that a dry patch with a given size to have a circular shape, and the occurrence of these patches alone was not sufficient to cause CHF. They also proposed that the temperature at the center of the dry patch first must reach a critical value above which liquid–solid contact was no longer possible. Once this condition occurs at a local point on the heating surface for most heat-flux-controlled systems, the dry patch starts growing, causing a dry patch finally to cover the entire heating surface, as the surface moved through transition boiling into film boiling. Unal et al. (1992) concluded that the occurrence of such a hot spot on the surface was the real cause of the CHF.

Carvalho and Bergles (1994) identified nucleate pool boiling sub-regimes together with the description of dry patch formation. They concluded that if the slope of the boiling curve was invariant, no dry patches were formed on the heating surface. And they believed, as proposed by Gaertner (1965), that the primary event for the onset of CHF was the propagation of dry patches or local dry areas or film boiling under vapor clots to envelop the whole heating surface. Nishio et al. (1998) observed the dynamic behavior of dry patches for the pool boiling of R-113 on a sapphire plate. They pointed out that the liquid–solid contact of the network pattern at CHF is much different from the observation of Gaertner, and the boiling structure model by Dhir and Liaw (1989) and Haramura and Katto (1983), in which isolated minute vapor stems are attached to the boiling surface.

Even though the dry patches were experimentally observed by a number of investigators as discussed above, they were not actively considered in CHF modeling so far. For example, Ha and No (1998a,b, 2000) successfully applied the behavior of dry patches to the development of CHF models. It seems evident that from the previous reviews that the bubble dynamics in each boiling sub-regime are closely related to the formation of dry patches that, at least, are responsible for the onset of the CHF. Therefore, to gain clear information for the CHF triggering mechanism, the simultaneous observation for the behaviors of bubbles and dry patches rather than the individual observation in the vicinity of a heating surface is essential.

Nishio et al. (1998) proposed a direct observation technique of the dynamic behavior of liquid–solid contact from below the boiling surface using a transparent boiling surface and optical measurements using a total reflection method. They proposed a new parameter describing the heat transfer in high-heat flux boiling based on experimental results obtained with the total reflection technique for pool boiling of saturated R-113 at atmospheric pressure. Nishio et al. (1998) termed the new parameter the "contact-line-length density" (CLLD) and was defined as the total length of contact-lines existing in unit area on the boiling surface. Nishio and Tanaka (2002) later proposed a simplified model to predict the CLLD at CHF based on optical images taken from below a boiling surface using a total reflection method. They also proposed a criterion to estimate the maximum value of the CLLD, where in this criterion it is assumed that CLLD reaches maximum value if the dry areas become to touch each other.

In a recent study by Chung and No (2003), new experimental using R-113 attempts were made to directly observe the physical boiling phenomena of bubbles and dry patches simultaneously from below a horizontal flat heating surface, whereas side views of bubbles were also attempted to obtain the two-dimensional bubble behavior. They observed that the formation of bubbles and dry spots occurs simultaneously. At CHF, the surface rewetting was repeated by the local nucleate boiling around the large vapor film. At post-CHF, nucleate boiling at the locally wetted region was extinguished, resulting in the dryout of the whole heating surface. Chung and No (2003) concluded that the CHF was triggered from the locally limited nucleate boiling activity rather than any hydrodynamic instability.

Several researchers investigated the effect of heating surface characteristics, such as surface configuration, thermophysical properties, wettability, roughness, geometry, and orientation, on nucleate pool boiling. For example, Rohsenow (1982) reported that changing surface characteristics can shift the position of the boiling curve markedly, because it tends to change the cavity size distribution. Nishikawa et al. (1984) proposed that the effects of surface roughness would be decreased if a system pressure was increased because active nucleation sites density on the heating surface was decreased with increasing pressure. Kang (2000) performed an experimental parametric study to investigate the effect of surface roughness on pool boiling heat transfer using saturated pool boiling of water at atmospheric pressure. He observed that an increase surface roughness tends to provide enhancement to heat transfer at a fixed wall superheat because the rough surface tends to have more cavities than the smooth surface, while pool boiling heat transfer coefficient depends on the nucleation site density. Kang (2000) also reported that an increase in surface roughness gives no observable change in pool boiling heat transfer characteristics, especially in high-heat flux region, for the horizontal tubes because of the lack in liquid agitation. However, its effect tends to magnify as the orientation of a tube changes from horizontal to the vertical position because the change in tube orientation gives much stronger liquid agitation and smaller bubble coalescence. Recently, Takata et al. (2005) performed an experimental study to investigate the effect of surface wettability on pool boiling at saturation conditions using a heating surface coated with a photocatalyst substance using titanium dioxide (TiO_2) that tends to have a high contact area with boiling water when irradiated by UV light. They observed that the TiO_2-coated surface exhibited higher heat transfer characteristics in nucleate boiling region and its CHF was higher than that obtained for the non-coated surface. Pioro et al. (2004) presented an extensive review on studies that investigated effects of boiling surface characteristics on nucleate pool boiling heat transfer. They reported that nucleate pool boiling is a very complicated process which is interdependently and simultaneously affected by heating surface characteristics under various boiling conditions.

3.1. Experimental techniques used for transient CHF

Flow transient CHF experiments are performed using electrically heated tubes (internal flow), single rod (annular flow or heated wire), or bundle of rods. Characterizing transient CHF requires determining important quantities at any time and along any location of the test section. These quantities are: heater temperature, pressure, mass flux, coolant enthalpy, and power to coolant. These important quantities are discussed in the following section.

3.1.1. Heater temperature measurement

Thermocouples are used to detect heated wall temperature at any location along the heater. The thermocouples are either directly attached to the heated wall through a metallic joint or through a dielectric joint such as mica, ceramic or even air. The response time of the thermocouples has an equal importance as that of accuracy when performing transient CHF experiments. The response time is an important parameter to determine the exact time at which CHF occurs from the recorded data. A too long time response could make the experiments meaningless except for very slow transients. Hassid (1973) suggests having a time response

of 0.2–0.4 s as satisfactory response. Direct attachment of the thermocouple junction to the metallic walls has been adopted by many researchers (e.g. Moxon and Edwards, 1967; Hicken et al., 1972). Very short time response can be obtained by this method (~0.1 s). Some of the drawbacks of using this technique arise from the difficulties of installation and the possibility of having electrical unbalance. Brazed sheathed thermocouples to the heated wall have been used by Gaspari et al. (1973). The results are satisfactory with an overall time response of 0.2–0.3 s. One other technique consists of silver soldering thermocouple junctions or sheath to a metallic piece fitted to the heated walls through an insulating layer. Hassid (1973) recommends that this method should be discarded due to the very large time response, unless when used for very slow transients.

3.1.2. Pressure measurement

The very large variety of available pressure transducers made the continuous measurement of pressure an easy task. The overall time response of the transducer-recording system must be specified. Determination of pressure at various locations along length is important when rapid pressure transients are expected (Gaspari et al., 1973).

3.1.3. Mass flow rate measurement

Mass flow rate determination is very difficult when two-phase flow is to be measured at both inlet and exit of the test section. The overall time response must be accurately determined, as emphasized by Moxon and Edwards (1967). Flinta et al. (1971) have proposed a continuous measuring technique based on the use of a turbine flow meter together with a "drag body meter". This method allows measuring mass flow as well as determining enthalpy. However, the reliability of this method is not fully established. Another technique has been used by Gaspari et al. (1973) and Agostini and Premoli (1971), which permits discrete measurements of mass balance over portions of the reactor or experimental test section coolant circuit. This method is based on a quick-acting valve technique (closure time $\leqslant$0.01 s). The drawback of this technique is that it requires many test repetitions. No attempts have been yet made to measure the mass flow rate at intermediate locations along the test section. From the available information it seems that much effort is still to be done, also for inlet and outlet flow measurements, which are very important parameters for the interpretation of transient CHF data.

3.1.4. Coolant enthalpy measurement

Temperature measurements of coolant are easier when a single phase fluid is present (sub-cooled liquid or superheated vapor). However, in the CHF transient, where two-phase flow is present, no information is in general available or reliable on coolant enthalpy. One of the suggestions to determine the coolant enthalpy during transients is through the measurement of void fraction which is related to quality, and therefore to enthalpy. It should be noted that the void fraction is normally expressed in terms of the slip velocity. The slip velocity is defined as the difference between the average velocities of two different fluids flowing together in a pipe. In vertical ascending flow, the lighter fluid flows faster than the heavier fluid. Also, the slip velocity depends mainly on the difference in density between the two fluids, and their holdups. Void fraction measurements are more reliable and accurate with the development of fiber-optics sampling techniques.

3.1.5. Power to coolant measurement

Determination of power to coolant is important in power and pressure transient tests. In these tests, power to coolant may be considerably different than generated power. Determination of power to coolant is also necessary when CHF is let to propagate upstream of the test section where temperature of the heater can vary considerably along its length (1973). This has a strong effect on generated power for heaters which have electrical resistance dependent on temperature. Thus a continuous measurement of current and voltage in a number of locations along length is in general useful.

4. CHF modeling studies

Most of the studies on CHF mechanism have been reviewed in numerous studies by Tong (1972), Tadreas and Kazimi (1990), Katto (1994), Collier and Thome (1996), and Tong and Weisman (1996). Furthermore, extensive research work has been made on modeling or experimentally describing the relevant physical processes leading to boiling crisis (Tong and Hewitt, 1972; Weisman and Ying, 1985; Hewitt and Govan, 1990; Galloway and Mudawar, 1993; Theofanous et al., 2002). Most CHF models are based on a description of a limiting process that limits flow to the heated surface during intense boiling. Galloway and Mudawar (1993) classified CHF modeling studies into three general categories: boundary layer separation models, bubble crowding models, and sub-layer dryout models. All three types of models were based on conditions that promote dryout of the heating surface, but differ in the physical description of the CHF triggering mechanism.

Sadasivan et al. (1995) reviewed the current status of CHF modeling and highlighted a number of areas where future CHF experiments should focus, and emphasized the need for new experiments towards further understanding of boiling crisis and CHF triggering mechanisms. Sadasivan et al. (1995) reported that the two main schools of thought that have emerged on the controlling mechanism of CHF were both based on the concept of hydrodynamic instability and the main difference between the two approaches is the location of the instability with respect to the heating surface. The hydrodynamic instability model, also termed as "far-field model", was originally presented in the foundation work of Zuber (1958) that was the first theoretical formulation of CHF. In this approach, CHF is triggered by the instability in the vapor–liquid interface of the vapor columns originating from the heating surface during the process of nucleate boiling. There, the onset of hydrodynamic instability leads to a breakdown in the process of vapor removal from the heating surface, leading eventually to entire vapor blanketing of the surface. In a heat-flux-controlled system, this causes the surface temperature to increase dramatically, whereas in a temperature-controlled system, this causes a slight reduction in the heat flux. Sadasivan et al. (1995) argued that because of the very nature of this model, the temperature of the heating surface does not play a role; CHF is solely a function of hydrodynamics of the vapor flow in the vapor columns above the heating surface. Sadasivan et al. (1995) also reported that based on the Zuber model the vapor flow from the heating surface is influenced by two major factors: the vapor generation at the heating surface as a result of the heat flux, and the vapor escape path or pattern from the heating surface. There, the heating surface geometry relates to CHF through its boiling area and the hydrodynamic flow pattern, which the given geometric configuration generates.

The Zuber model was first used to predict CHF in saturated pool boiling over horizontal surfaces, such as infinite flat plate. The model was then used to evaluate CHF in a variety of pool boiling situations depending on appropriate configuration-related modifications. For example, Lienhard and Dhir (1973) further developed the Zuber model and used it to predict CHF on wires, ribbons, etc. Lienhard (1988) reviewed studies that utilized the Zuber model to predict burnout on cylinders taking into accounts such variables as size, properties of the boiled liquid, gravity, liquid subcooling, velocity of an imposed cross flow, and certain other vari-

ables as well. Dhir (1991) reviewed studies that provided mechanistic understanding, including the Zuber model, of nucleate and transition boiling heat transfer under pool and external flow boiling conditions. Katto (1994) presented an extensive review of experimental and theoretical studies on CHF phenomenon under various geometrical configurations and boiling conditions, including a survey of a number of fundamental models of CHF and transition boiling, such as the Zuber model.

Kirby and Westwater (1965) and Yu and Mesler (1977) reported the existence of a thin-rich liquid sub-layer between the large vapor mushrooms and the heating surface. The possible role of this so-called macro-layer in nucleate boiling and CHF was not explored in detail for several more years. In 1983, Haramura and Katto (1983) proposed the "macro-layer" dryout model, also termed as "near-surface model", based on series of experimental observations including Gaertner's (1965), which seem much different from the physical model used by Zuber (1958). The macro-layer dryout model postulates that the macro-layer formed on the heating surface with an initial thickness is evaporated away during a hovering period of the overlying vapor mass when the CHF appears. The macro-layer model still retained the basic element of the Zuber model, i.e. hydrodynamic instabilities control the occurrence of CHF, but based on the condition of the dryout of the macro-layer without liquid resupply throughout the period of vapor mushroom. Haramura and Katto (1983) proposed that the controlling instabilities occur not at the walls of the vapor columns as envisioned by Zuber (1958) but rather at the walls of the minute vapor stems around active nucleation cavities that intersperse the liquid macro-layer at the heating surface.

On-wall mechanisms are not considered in either of the two above models. Some attempts have been made to explain the detailed processes of heat and mass transfer on the heating surfaces. A group of studies have been performed by Pasamechmetoglu et al. (1993) based on the macro-layer dryout model, in which the dominant heat transfer is attributed to the evaporation at the liquid–vapor–solid contact points. Another group of studies have been performed by Dhir and Liaw (1989) who proposed the "unified model" for CHF, in which the heat flux is related to the void fraction and. Furthermore, Lay and Dhir (1995) have proposed a vapor stem model and made a dynamic analysis of it, from which stable minute vapor stems are possible. Those models have shown that only the evaporation of a so-called micro-layer (which is much thinner than the macro-layer) can contribute to the high-heat flux in fully developed nucleate boiling. Extensive studies have been performed to understand these complex transport processes, but due to experimental difficulties only a few studies have focused on the micro-phenomena of such processes. For example, Moore and Mesler (1961) deduced the existence of micro-layer from observations of rapid fluctuations in the temperature of a heating surface on which bubbles were being generated. The existence of a thin evaporating micro-layer beneath a growing bubble in nucleate pool boiling was then experimentally confirmed by Cooper and Lloyd (1969), and it was observed that the evaporation of the micro-layer contributed significantly to the growth of the bubbles.

Cooper (1969) developed a micro-layer theory to predict the growth of bubbles in nucleate pool boiling. Judd and Hwang (1976) studied the role of micro-layer evaporation mechanism in nucleate pool boiling heat transfer. They performed a comprehensive set of measurements that substantiated a model for the prediction of boiling heat flux that incorporated micro-layer evaporation, natural convection, and nucleate boiling mechanisms. Judd and Hwang (1976) also found that the micro-layer evaporation heat transfer represented a significant proportion of the total heat transfer for the range of heat flux considered. Haider and Webb (1997) reported that the high-heat flux in nucleate boiling can be attributed to one or more of the following possible mechanisms: (1) transient conduction, and subsequent replacement of, the superheated liquid layer in contact with the heating surface, (2) evaporation of a thin liquid micro-layer beneath the growing bubble, and (3) circulation of liquid in the vicinity of a growing bubble due to thermocapillarity effects at the vapor–liquid bubble interface. Many of experimental studies indicated that the boiling curve around the CHF point is a continuous function of wall superheat and the boiling mechanism does not change drastically at CHF (Nishio and Tanaka, 2002). However, it is expected that vapor and liquid transport balances would change.

Zhao et al. (2002a,b) proposed a new dynamic micro-layer model to predict theoretically CHF in transient and fully developed nucleate boiling regions for pool boiling on horizontal surfaces. Their experimentally-validated model presented a dynamic structure of vapor–liquid–solid contacts and the boiling heat transfer was mainly attributed to the evaporation of the micro-layer which was formed during the initial growth period of individual bubbles. In their model, the micro-layer thickness and the dryout area as well as the wall heat flux were formulated as functions of wall superheat. They also found that the initial thickness of the micro-layer becomes thinner with increasing of wall superheat, and both the evaporation and the partial dryout speed of the micro-layer increase.

4.1. Modeling aspects related to transient CHF

It should be noted that the analysis of transient CHF data is based mostly on the use of computer codes for calculation of flow and enthalpy transient at any location along the heated length. These codes are developed to solve mass, momentum and energy balance equations together with some steady-state empirical correlations for the calculation of quantities such as slip ratio (void fraction), heat transfer coefficient, pressure drop, etc.

Some of the attempts were made to predict transient CHF from inlet conditions (Moxon and Edwards, 1967; Hein and Mayinger, 1972). The results of using inlet conditions were unsatisfactory which led to the adoption of using local instantaneous conditions for predicting transient CHF. Generally the time at which CHF occurs for any location along the test section is calculated using a steady-state correlation. Basically there are two different approaches for steady-state correlations used:

- correlations of the form (e.g. Morgan et al., 1972; Moxon and Edwards, 1967; Hein and Mayinger, 1972):

$$q = q(X, G, P) \tag{3}$$

  where q is the heat flux to coolant which is considered as a unique function of the local quality X, the local mass flux G, and the local pressure P, and
- correlations of the form (e.g. Gaspari et al., 1973):

$$X = X(L_H, G, P) \tag{4}$$

  where X is the local quality which is considered to be a unique function of heated length L_H, local mass flux G, and local pressure P. The comparison between experimental transient CHF data and predictions from analytical models is usually performed on the time at which CHF occurs from the beginning of the transients (e.g. Gaspari et al., 1973; Tong et al., 1965).

Two major concerns are worth mentioning in performing the analysis. The first concern is the reliability of overall comparison is dependent on the computer code to predict local and instantaneous values of flow and temperature (or enthalpy), and the CHF steady-state correlation at the mass flow rate,

pressure, quality and heat flux (or length) for which CHF occur. The second concern arises in performing the comparison on critical heat flux considered to be more significant than on the time at which CHF occurs (Hassid, 1973). A better agreement will be achieved when the accuracy of transient CHF prediction is comparable to that required for a steady-state CHF correlation. This is better evidenced if critical heat flux is considered.

In conclusion, the general approach to predict transient CHF is to relate it to corresponding steady-state CHF values obtained at the same instantaneous local pressure, mass flux and quality (quasi-steady-state approach),

$$K_{TR} = \frac{q_{CHF,TR}}{q_{CHF,SS}} \tag{5}$$

In the above Eq. (5), transient CHF, $q_{CHF,TR}$, is obtained directly from the experiment. However there are three ways applied to obtain the steady-state CHF, $q_{CHF,SS}$ namely:

(a) by obtaining steady-state CHF experimental data with flow conditions matching the corresponding instantaneous local conditions of the transient CHF,
(b) by curve-fitting of the steady-state CHF data for the same range of conditions of transient CHF data, and use the curve-fit to predict steady-state CHF values, or
(c) by using very well established steady-state CHF correlations like the ones used in safety codes.

5. Transient CHF experiments

5.1. Flow transient experiments

Table 2 lists the ranges of conditions of flow transient experiments reviewed in this study. Experiments on flow transients are divided into two types: (a) flow decay (including flow oscillation) and (b) flow stoppage (sudden LOCA) experiments. Flow stoppage experiments are in general more significant than flow decay (Hassid, 1973), since all the involved phenomena are of dynamic nature. These experiments are valuable to understand the basic mechanisms of CHF onset in transients and to check the validity of the analytical models. Moreover, flow stoppage transients are also connected to BWR LOCA transients, where inlet flow is assumed to be instantaneously lost due to the jet pumps being uncovered.

Moxon and Edwards (1967) suggested that the local CHF mass velocity tends to be lower in a transient situation than under steady-state conditions. However, the majority of studies indicate that, although the CHF mass velocity at the inlet decreases in fast transient, the occurrence of CHF could be estimated well from the instantaneous local conditions at the CHF location with steady-state correlations (Leung et al., 1981).

Smirnov et al. (1973) conducted flow transients in a single tube (0.5 and 1.4 m long) with flow decreased by 40–70% of its initial value within 0–3 s. Instantaneous local parameters of flow of CHF were determined by calculation. Steady-state CHF was obtained

Table 2
Flow transient experiments.

Reference	Fluid	Test section geometry	Flow conditions	Transient
Smirnov et al. (1973)	Water	One tube	9.7 MPa 1000–3000 kg m^{-2} s^{-1} 280–340 kW m^{-2}	Flow decay
Hein and Mayinger (1972)	Water	One tube, one annulus, 4- and 9-rod bundles	6.9, 13.8 MPa 1360 kg m^{-2} s^{-1} 1420 kW m^{-2}	Power ramp, flow decay
	R-12		1.1 MPa 500–3500 kg m^{-2} s^{-1} 320 kW m^{-2}	Power ramp, flow decay
Gaspari et al. (1973)	Water	One annulus outer tube heated,	4.9 MPa 136–2710 kg m^{-2} s^{-1} 240–830 kW m^{-2}	Flow stoppage
		One tube, both 4 m long	4.9 MPa 680–1500 kg m^{-2} s^{-1} 350–830 kW m^{-2}	Exponential power ramp
Shih (1974)	R-11	One annulus inner rod heated 0.92 m heated	0.95–1.13 MPa 380–760 kg m^{-2} s^{-1} 95–126 kW m^{-2}	Flow decay and surge with power ramp or decay
Zielke and Wilson (1974)	Water	9-Rod bundle, 1.83 m long	15.2 MPa 1360–4070 kg m^{-2} s^{-1} –	Power ramp, flow decay
Celata et al. (1986a,b)	R-12	Round tube ID = 7.5 mm L = 2300 mm	1.2–2.75 MPa 1000–1470 kg m^{-2} s^{-1} 32–85 kW m^{-2}	t_h = 0.4–10.0 s
Sugawara and Shiba (1987)		36-Rod bundle L = 3.7 m	2–7 MPa 10–50 Ton h^{-1} per bundle 2–6 MW m^{-2}	Flow reduction rate up to 500% s^{-1}
Iwamura and Kuroyanagi (1982)	Water	Round tube ID = 10 mm L = 800 mm	0.5–3.9 MPa 1240–3050 kg m^{-2} s^{-1} 2160–3860 kW m^{-2} T_{in} = 210 °C	Flow reduction rate = 0.6–35% s^{-1}
Lee and Lin (1993)	Water	Round tube, 3.6 m ID = 13.4 mm	6.9, 15.5 MPa 1960–3800 kg m^{-2} s^{-1} 1.1–1.46 MW m^{-2}	Flow reduction rate = 0.1–30% s^{-1}
Iwamura et al. (1994a,b)	Water	Triangular-pitch 7-rod OD = 9.5 mm (heater rod) Rod pitch = 11.7 mm	P_0 = 13.0–15.5 MPa G_0 = 2000–3200 kg m^{-2} s^{-1} T_{in} = 260–310 °C	Flow reduction rate = 1.6–30% s^{-1}

in the same test section. With a sharp decrease in mass velocity the computed time to CHF was sooner than experimentally observed which implies that the transient CHF was higher than the steady-state CHF.

Hein and Mayinger (1972) summarized the power and flow transient test results conducted in a single tube, an annulus, 4-rod and 9-rod bundles. Results showed improvement (conservative prediction) over steady-state CHF levels with linear power-excursion time of a few seconds. For flow transients, good agreement was obtained between transient and steady-state CHF. Only at very low mass flux the CHF improvement occurred, which was attributed this to the finite time required for complete evaporation of the liquid film on the heated surface.

Gaspari et al. (1973) used a directly heated annular test section cooled by 5 MPa water to measure the time to dryout for inlet flow stoppages (at constant pressure and power). It was concluded that the steady-state CHF correlations can be used to predict the transient time to dryout for the described flow conditions.

Shih (1974) extended Ahmad's (1973) compensated distortion scaling model to predict transient CHF in an annular test section utilizing Freon-11 as the working fluid. More distortion parameters were introduced to meet requirements in the various transients, and these parameters were determined experimentally. Then different transient conditions were scaled up to equivalent conditions in the water system and simulated by a computer code. In the flow transients, the inlet flow was reduced by 1/3 in about 1.5 s and CHF occurred long after (~1.5 s) the mass velocity has established in a stable but lower flow configuration. In all cases, no CHF was observed while the flow was decaying. However, the onset of CHF was well predicted the code to within ±20%.

Celata et al. (1986a,b) conducted experiments of R-12 flow boiling in a tube of 7.5-mm ID and 2300 mm long at 1.25–3.00 MPa (covering PWR and BWR conditions with respect to equal density ratio) and mass flux of $G = 1.01–1.47$ Mg m^{-2} s^{-1}. They measured the time interval from the start of the flow transient to the onset of the CHF. The steady-state CHF correlations were found to be inadequate in accurately predicting the onset of the CHF in the case of a fast flow transient (half-flow decay time $t_h < 5.0–6.0$ s) and with reasonable accuracy of prediction for slower transients. Celata et al. (1986a,b) showed that the steady-state CHF correlations conservatively predicted transient CHF values ($q_{CHF,TR} > q_{CHF,SS}$).

Sugawara and Shiba (1987) performed flow transient tests in a 36-rod bundle, operating at ~7 MPa and initial flows of 1.5–2.0 Mg m^{-2} s^{-1} and flow reduction rate of 0–500% s^{-1}. No effect on the CHF was observed for the range of flow reduction rate.

Iwamura and Kuroyanagi (1982) experimented on the CHF in transients caused by a linear reduction in the mass flow rate under constant pressure and heat flux. Tests were carried out for water boiling at 0.1–3.9 MPa in either a tube (10 mm ID and 800 mm long) or annuli (a heated inner tube of 10 mm OD and 800 mm long with a glass shroud of 12.8–14.0 mm ID). The observations suggested that the CHF was caused by the "dryout of a liquid sublayer" on the heated surface, and a method was proposed to predict the transient time before the onset of the CHF based on the local conditions. In subsequent work, Iwamura et al. (1994a,b) obtained transient CHF values in a 7-rod assembly having a cosine AFD, at PWR conditions of interest ($P = 13.0–15.0$ MPa, $G = 2.0–3.2$ Mg m^{-2} s^{-1}) with flow decreases up to −30% s^{-1}. For the comparison between transient and steady-state CHF values, Iwamura et al. (1994a,b) used steady-state correlations having 10% uncertainty with steady-state data obtained by the same test section. Transient CHF values were accurately predicted by the steady-state CHF correlations (within the uncertainty range).

Lee and Lin (1993) performed experiments on a single tube to cover the flow conditions of both BWR and PWR for flow reduction rates up to 30% s^{-1}. They also investigated experimentally the effect of transient speed on the local mass velocity. The effect was found to be very small. Lee and Lin applied different steady-state correlations to predict transient CHF with and without the correction factor of Chang et al. (1989). Lee and Lin (1993) concluded that the local condition approach can be applied in the predictions of flow transient CHF for the range under investigation.

5.2. Power transient experiments

The ranges of power transient experimental conditions reviewed in this study are listed in Table 3. Zielke and Wilson (1974) reported power transients performed on a 1.83 m long, 9-rod bundle. Typical reactor power ramp was simulated. Transient CHF values were predicted using the steady-state correlation with about 5% in the conservative side.

Aoki et al. (1976) made extensive studies of transient heat input in an annulus. The observed behavior of transient CHF was determined according to three regions of flow conditions. At high flow (mass flux around 2.1 Mg m^{-2} s^{-1}) and large sub-cooling, CHF levels appear to be independent of power ramp rate. In the second region, where CHF occurs at 50–70% void fraction, the transient CHF follows the steady-state value closely. Because of the moderate void fraction, the bulk conditions affect the heat transfer at the surface. For the third region, where CHF caused by dryout occurs slowly, the transient CHF levels appear to increase with increasing power ramp rate.

Pasamehmetoglu et al. (1990) performed analytical study on the effect of power transients on CHF in flow boiling. Quasi-stea-

Table 3
Power transient experiments.

Reference	Fluid	Test section geometry	Flow conditions	Transient
Zielke and Wilson (1974)	Water	9-Rod bundle, 1.83 m long	15.2 MPa 1360–4070 kg m^{-2} s^{-1} –	Power ramp
Aoki et al. (1976)	Water	One annulus inner rod heated 0.1, 0.5 m heated	2.1–7.0 MPa Up to 2100 kg m^{-2} s^{-1}	Power ramp to max 6000 kW m^{-2}
Sugawara and Shiba (1987)		36-Rod bundle$L = 3.7$ m	2.0–7.0 MPa 10.0–50.0 Ton h^{-1} per bundle 0.5–5.5 MW	Power increase rate up to 500% s^{-1}
Iwamura et al. (1994a,b)	Water	Triangular-pitch 7-rod OD = 9.5 mm (heater rod) Rod pitch = 11.7 mm	13.0–15.5 MPa 1430–2400 kg m^{-2} s^{-1} T_{in} = 291–310 °C	Power increase rate of 2.0–120% s^{-1}
Inoue et al. (2000)	Water	Heater block with length 4.8–65.0 mm and surface curvature of 24.8, 62.1, ∞ mm	Jet velocity = 1.1, 2.5, 5.0, 8.0, 12.0 m s^{-1} Subcooling = 30, 60, 80 K Up to 50 MW m^{-2}	Power input rate of 1.1, 2.5, 10.0 MW m^{-2} m s^{-1}

dy-state approach was applied in the analysis with the use of Kataoka et al. (1983) transient data for the comparison. Excellent agreement was obtained between the predicted and experimental CHF values.

Sugawara and Shiba (1987) performed power transient tests in a 36-rod bundle, operating at ~7 MPa and initial flows of 1.5–2.0 Mg m^{-2} s^{-1} and heat flux increase rate of 0–500% s^{-1}. Transient CHF was equal to steady-state CHF for heat flux increase rate up to 0.5 MW m^{-2} s^{-1}. Transient CHF was higher at higher heat flux increase rates.

Iwamura et al. (1994a,b) obtained transient CHF values in a 7-rod assembly having a cosine AFD, at PWR conditions of interest (P = 13.0–15.0 MPa, G = 1.43–2.40 Mg m^{-2} s^{-1}) with simultaneous power increases of up to +120% s^{-1}. For the comparison between transient and steady-state CHF values, Iwamura et al. (1994a,b) used steady-state correlations having 10% uncertainty with steady-state data obtained by the same test section. Transient CHF values were predicted accurately by the steady-state CHF correlations (within the reported uncertainty range).

Inoue et al. (2000) studied the effect of power transient on cooling fusion reactor by impinging planar jet flow using ramped power input. Steady-state CHF data were obtained in the same testing facilities for comparison. Inoue et al. (2000) found that the transient CHF is equal to or higher than steady-state CHF and the difference in values increases with increasing the heat input rate.

As a summary of the effect of power transient on CHF, the time at which CHF occurs can be predicted quite accurately through local and instantaneous values, calculated through computer codes. The agreement between prediction and experimental data is equivalent to that found in flow transient tests and, in terms of critical heat flux, it is within the accuracy usually accepted for steady-state CHF prediction.

5.3. Pressure transient experiments

The reported information on pressure decay transients is much less than for flow and power transients. Experiments have been carried out at constant or variable power transients (power-to-coolant varies during the transient, because of saturation temperature decrease) and with different flow transients (Table 4). Flow measurements in these transients are very difficult because two-phase flow occurs when saturation conditions are reached.

Cermak et al. (1970) performed blow-down tests with exit break in a 21-rod PWR bundles from an initial pressure of 10.3 MPa. Steady-state CHF data conducted in the same bundle were used to predict the transient CHF, together with instantaneous local conditions. t_{CHF} was reported to be affected by the depressurization rate and the prediction under estimated t_{CHF} by as much as 5.7 s for an actual observed t_{CHF} of 7 s. In six other tests CHF were predicted to occur within the first 5 s but was not observed experimentally. Cermak et al. (1970) conclusion was that CHF during blow-down could be conservatively predicted on the basis of steady-state data.

Lawson (1971) reported blow-down results in both single rod and 7-rod bundles with an exit break. From an initial pressure of 10.3 MPa, the pressure transient lasted from 12 to 60 s. No CHF was observed in the tests reported until the test section was at (or near) atmospheric pressure and the coolant was almost depleted. The effect of flow reversal, resulting from an inlet break was studied too with the single 3.66 m rod enclosed by an outer unheated shroud with a chopped cosine power profile and a peaking factor of 1.69. About thirty blow-down tests were performed and the earliest t_{CHF} was about 4 s. Also it was found that for break areas greater than 1.9 cm^2, t_{CHF} decreases with increasing break area. At smaller break areas, t_{CHF} begins to decrease with decreasing break area. Further in the small-break regime, CHF occurred at considerably higher pressures than in the large-break regime. It was suggested that CHF was a dryout phenomenon in large-break tests and possibly a departure from nucleate boiling phenomenon in small-break tests.

Hicken et al. (1972) studied the effect of break area, and the heat flux in a single tube during blow-down from an initial pressure of 9.0 MPa. Pressure decay was found to be faster with larger break orifices as expected. A rise in system pressure was observed for small breaks as a result of the volumetric vapor-generation rate exceeding the discharge mass flow rate. Their findings in transient CHF can be summarized as follows:

- t_{CHF} decreased with increasing heat flux,
- t_{CHF} decreased downstream for large heat flux, but this dependency was small at low flux,
- with large upstream breaks (with flow reversal), t_{CHF} was short for large heat flux but the upper region of the test section did not experience early CHF,
- t_{CHF} for double-ended breaks was intermediate between the times for single ended breaks.

Shih (1974) extended Ahmad's (1973) compensated distortion scaling model to predict transient CHF in an annular test section utilizing Freon-11 as working fluid. More distortion parameters were introduced to meet requirements in the various transients, and these parameters were determined experimentally. Then different transient conditions were scaled up to equivalent conditions in the water system and simulated by a computer code. Shih (1974) reported eleven depressurization transients. The system pressure decayed from 1.12 MPa to 0.89 MPa in 1–4 s, equivalent to the pressure range from 6.9 MPa to 5.52 MPa in water system. Onset of CHF ranged from 1.0 to 4.3 s, after the pressure had reached its minimum value in most cases. The predictions from

Table 4
Pressure transient experiments.

Reference	Fluid	Test section geometry	Flow conditions	Transient
Cermak et al. (1970)	Water	21-Rod bundle 1.53 m heated	10.34 MPa 1350–4070 kg m^{-2} s^{-1} 1900–3160 kW m^{-2}	Exit break
Lawson (1971)	Water	1-Rod in annulus, and 7-rod bundle, both 0.61 m heated	10.34 MPa 1350 kg m^{-2} s^{-1} 1100 kW m^{-2}	Exit break
Hicken et al. (1972)	Water	Single tube, 3 m heated 13.8 mm ID	9.0 MPa – 1650 kW m^{-2}	Inlet break, exit break Double-ended break
Shih (1974)	R-11	1-Rod in annulus, 0.92 m heated, 15.9 mm rod OD	1.12 MPa 390–660 kg m^{-2} s^{-1} 100–140 kW m^{-2}	De-pressurization by throttling

Table 5
Combined transient experiments.

Reference	Geometry	Fluid	Flow conditions	Transient
Celata et al. (1989)	Round tube D = 7.7 mm L = 2.3 or 1.18 m	R-12	1.2, 2.75 MPa 1030–1500 kg m^{-2} s^{-1} ΔT_{in} = 23–0 °C t_h = 0.4–7.0 s Margin to dryout = 0.5, 1.7 kW	Flow and power (ramp and step)
Celata et al. (1991)	Round tube	R-12	1.25, 2.02 MPa 1470 kg m^{-2} s^{-1} ΔT_{in} = 23–0 °C t_h = 0.5 s dp/dt = 0.02–0.3 MPa s^{-1}	Flow and pressure
			2.02 MPa 1470 kg m^{-2} s^{-1} ΔT_{in} = 23–0 °C t_h = 0.4 s dp/dt = 0.02–0.3 MPa s^{-1} Margin to dryout = 0.5, 1.7 kW	Pressure and power (step and ramp)
	D = 7.7 mm L = 2.3 or 1.18 m		1.25, 2.02, 2.77 MPa 1470 kg m^{-2} s^{-1} ΔT_{in} = 23–0 °C t_h = 0.4 s dp/dt = 0.06–0.32 MPa s^{-1} Margin to dryout = 0.5, 1.7 kW	Flow, pressure and power (step and ramp)
Iwamura et al. (1994a,b)	Triangular-pitch 7-rod OD = 9.5 mm (heater rod) Rod pitch = 11.7 mm	Water	15.5 MPa 2000–3200 kg m^{-2} s^{-1} T_{in} = 291 °C Flow reduction rate = 2.2–25% s^{-1} Power increase rate = 2.5–75% s^{-1}	Flow and power

the computer code were not as good as the flow transients since one dimensionless parameter was unable to be matched in his scaling process.

5.4. Simultaneous transient experiments

The ranges of experimental conditions investigated for combined transient experiments are listed in Table 5 along with the types of transients of each experiment. Celata et al. (1988, 1989) studied the CHF during transients caused by simultaneous changes in the flow rate and thermal power (for an exponential decrease in the mass flow rate and ramp – and stepwise increases in power) under constant pressure condition. Then, Celata et al. (1991, 1992) studied the CHF in the case of transients caused by simultaneous variations in either two or three of the parameters pressure, mass flow rate and thermal power (an exponential decrease in pressure, an exponential decrease in flow rate and ramp – and stepwise increases in power). In the two studies, the analyses were conducted on the basis of the local conditions hypothesis as well as the quasi-steady-state assumption. In all cases, the time to dryout was greater for the transients than for the steady-state; hence the transient CHF was higher than the corresponding steady-state case (conservative).

Iwamura et al. (1994a,b) obtained transient CHF values in a 7-rod assembly having a cosine AFD, at PWR conditions of interest (P = 15.0 MPa, G = 2.0–3.0 Mg m^{-2} s^{-1}) with simultaneous power increases of up to +75% s^{-1} and flow decreases up to –25% s^{-1}. For the comparison between transient and steady-state CHF values, Iwamura et al. (1994a,b) used steady-state correlations having 10% uncertainty with steady-state data obtained by the same test section. Transient CHF values were accurately predicted by the steady-state CHF correlations (within the uncertainty range).

6. Analysis of reported results in the literature

Two groups of data were extracted (digitized) and presented here. Other data were either difficult to extract or difficult to analyze. For the non-included data, the conclusions from the source are used to determine the range of application of the steady-state correlations to predict transient CHF.

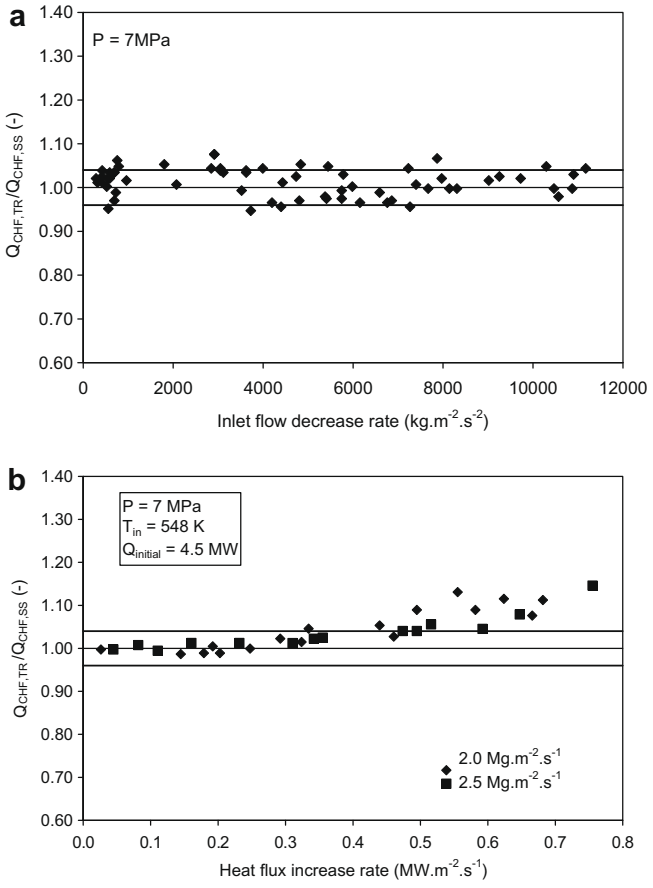

Fig. 2. Presentation of Sugawara and Shiba (1987). (a) Flow transient data and (b) power transient data.

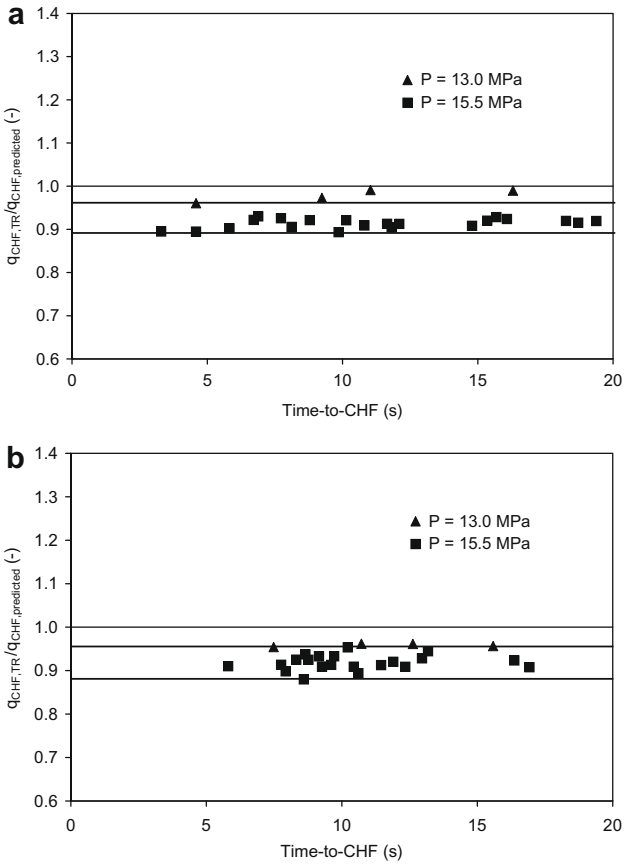

Fig. 3. Transient data of Iwamura et al. (1994a,b). (a) Flow transient and (b) power transient data.

The experiment of Sugawara and Shiba (1987) was performed on a full-scale bundle to cover flow and power CHF transients. The results were compared with steady-state prediction method derived from experimental data obtained in the same loop. The results of flow and power transients are shown in Fig. 2 along with the uncertainty of the used steady-state correlation (±4%). The flow transient CHF is very well predicted by the steady-state correlation while the power transient CHF starts to deviate at higher transient speeds. Even with this deviation, one can see improvements in transient CHF values over the steady-state values.

Fig. 3 shows the transient CHF data of Iwamura et al. (1994a,b). Both steady-state and transient CHF experiments were performed in the same experimental facility. The uncertainty of steady-state correlation used in the analysis is also shown in Fig. 3 (the two lines below unity). Although there is a bias in the prediction of the steady-state data, the same bias appears in predicting the transient CHF data. Taking this into considerations, there is an excellent agreement between transient CHF and the prediction of the steady-state correlation.

Much of the knowledge and understanding of the complex behavior of boiling phenomena have come from direct visualization and observation of such systems. As a classical visualization study, Gaertner (1965) performed a photographic observation of nucleate boiling on a horizontal surface and directly visualized the boiling phenomena in the near-wall region. Gaertner (1965) hypothesized the second transition region, where the stems of the vapor mushrooms collapse causing local vapor patches to form on the heating surface. He concluded that widespread vapor patches caused boiling crisis. More recently, many investigators have used high-speed visualization as a tool to study boiling crisis characteristics, and to qualify and quantify the relative contributing factors to the high-heat flux in nucleate pool boiling (Han and Griffith, 1965; Sun and Lienhard, 1970; Paul and Abdel-Khalik, 1983; Arshad and Thome, 1983; Chien and Webb, 1998; Nishio et al., 1998; Ramaswamy et al., 2002; Pascual et al., 2002; Chung and No, 2003; Nishio and Tanaka, 2004). However, the characteristics of boiling that make optical techniques attractive also entail difficulties in their application. Kenning (2004) reported that depending on boiling conditions, boiling phenomenon is normally accompanied by high-heat fluxes at boundaries, causing large gradients of refractive index in the liquid that deflect light rays, which are also absorbed by the liquid and refracted and reflected at many liquid–vapor interfaces. This tends to limit the distance over which optical observation can be made in the boiling system. Kenning (2004) also reviewed many experimental studies that used optical measurement techniques to observe boiling phenomenon and CHF mechanisms. He reported some insights and limitations with respect to optical techniques used in boiling heat transfer and CHF experiments for pool and forced convective boiling applications.

7. Conclusion and recommendations for future work

Despite extensive theoretical, modeling and experimental efforts, there are still substantial differences regarding boiling characteristics and CHF triggering mechanisms, and knowledge of the precise nature of CHF is still not well understood. This is mainly due to the very complex nature of boiling phenomenon as reported by Katto (1994). The disagreements in describing the boiling crisis come primarily from the lack of in-depth knowledge of the physical phenomena causing CHF on the near-wall region of the heating surface. Consequently, the majority of CHF models developed to this point were based on postulated mechanisms, which were not verified through direct observation due to difficulties in performing detailed flow visualization of the near-wall region at a heat flux approaching CHF. Hence, in order to accurately describe CHF triggering mechanisms, direct observation of the on-wall and near-wall regions during boiling crisis is deemed very important.

The observed effect of flow transient on CHF can be summarized as follows: t_{CHF} can be predicted quite accurately through parameters calculated by means of computer codes and steady-state correlations. Two kinds of steady-state correlations have been used in the literature based on the local values of heat flux, quality and flow rate and based on the local values of quality, flow rate and boiling length. The results are almost equivalent and the agreement between prediction and experimental data is equivalent to the accuracy usually accepted for CHF steady-state correlations.

Some difficulties arise when CHF occurs at high quality and/or low flow rate, since only special correlations are suitable in this range. However, it should be concluded that no enough work has been done to investigate the combined transient effects on CHF. From the very limited available studies it is most likely applicable to use the steady-state correlations to predict transient CHF. The prediction in this case is considered to be conservative.

Acknowledgments

The authors would like to thank the Deanship of Scientific Research (DSR) at King Fahd University of Petroleum and Minerals for their support in order to perform this work.

References

Agostini, V., Premoli, A., 1971. Valvla di Intercettazione Rapida per Impiego in Aqua Vapore. Energia Nulearo 8.

Ahmad, S.Y., 1973. Fluid to fluid modeling of critical heat flux: a compensated distortion model. Int. J. Heat Mass transfer 16, 641–662.
Aoki, S., Kozawa, Y., Iwasaki, H., 1976. Boiling and burnout phenomena under transient heat input. Bull. JSME 19, 667–675.
Arshad, J., Thome, J.R., 1983. Enhanced boiling surfaces: heat transfer mechanism and mixture boiling. In: Proceedings of the of ASME–JSME Thermal Engineering Joint Conference, vol. 1, pp. 191–197.
Barthau, G., Hahne, E., 2004. Experimental study of nucleate pool boiling of R-134a on a stainless steel tube. Int. J. Heat Fluid Flow 25, 305–312.
Browne, M.W., Bansal, P.K., 1999. Heat transfer characteristics of boiling phenomenon in flooded refrigerant evaporators. Appl. Therm. Eng. 19, 595–624.
Carvalho, R.D.M., Bergles, A.E., 1994. The pool nucleate boiling flow patterns of vertically oriented, small heaters boiling on one side. In: Proceedings of the 10th International Heat Transfer Conference, Brighton, UK, vol. 5, pp. 25–30.
Celata, G.P., Cumo, M., Annibale, F.D'., 1986. Critical heat flux in flow transients. In: Proceeding of the 8th International Heat Transfer Conference, San Francisco, vol. 5, pp. 2429–2435.
Celata, G.P., Cumo, M., Annibale F.D'., 1986, CHF in flow boiling during pressure transients. In: Proceedings of the 4th Miami International Symposium on Multi-Phase Transport & Particulate Phenomena, Miami Beach, Decembre, 1986.
Celata, G.P., Cumo, M., Anniblale, F.D'., Farello, G.E., SAID, S.A., 1988. Critical heat flux phenomena in flow boiling during step-wise and ramp-wise power transients. Rev. Gen. Therm. 317, 296–303.
Celata, G.P., Cumo, M., Anniblale, F.D'., Farello, G.E., 1989. Critical heat flux in transient flow boiling during simultaneous variations in flow rate and thermal power. Exp. Therm. Fluid Sci. 2, 134–145.
Celata, G.P., Cumo, M., Annibale, F.D'., Farello, G.E., Mariani, A., 1991. CHF behaviour during pressure, power and/or flow rate simultaneous variations. Int. J. Heat Mass Transfer 34, 723–738.
Celata, G.P., Cumo, M., Annibale, F.D'., Farello, G.E., 1992. A data set of critical heat flux of boiling R-12 in uniformly heated vertical tubes under transient conditions. Exp. Therm. Fluid Sci. 5, 78–107.
Cermak, J.O., Farman, R.F., Tong, L.S., Casterline, J.E., Kokolis, S., Matzner, B., 1970. The DNB in rod bundles during pressure blowdown. J. Heat Transfer 92, 621.
Chan, A.M.C., Shoukri, M., 1987. Boiling characteristics of small multitube bundles. ASME J. Heat Transfer 109, 753–760.
Chang, S.H., Lee, K.W., Groeneveld, D.C., 1989. Transient-effects modeling of critical heat flux. Nucl. Eng. Des. 133, 51–57.
Chen, J., Liao, J., Kuang, B., Zhao, H., Yang, Y., 2004. Fluid-to-fluid modeling of critical heat flux in 4×4 rod bundles. Nucl. Eng. Des. 232, 47–55.
Cheng, S.C., Doerffer, S., Tain, R.M., Hammouda, N., Huang, X.C., 1993. Experimental and analytical fluid-to-fluid modeling studies. Final Report No. C83041 Under Contract with Atomic Energy of Canada Ltd., (AECL).
Chien, L.-H., Webb, R.L., 1998. Measurement of bubble dynamics on an enhanced boiling surface. Exp. Therm. Fluid Sci. 16, 177–186.
Chiou, C.-B., Lu, D.-C., 1997. Pool boiling of R-22, R-124 and R-134a on a plain tube. Int. J. Heat Mass Transfer 40, 1657–1666.
Chung, H.J., No, H.C., 2003. Simultaneous visualization of dry spots and bubbles for pool boiling of R-113 on a horizontal heater. Int. J. Heat Mass Transfer 46, 2239–2251.
Collier, J.G., Thome, J.R., 1996. Convective Boiling and Condensation, third ed. Oxford University Press Inc., New York, NY.
Cooper, M.G., 1969. The microlayer and bubble growth in nucleate pool boiling. Int. J. Heat Mass Transfer 12, 915–933.
Cooper, M.G., Lloyd, A.J.P., 1969. The microlayer in nucleate pool boiling. Int. J. Heat Mass Transfer 12, 895–913.
Cornwell, K., 1990. The influence of bubbly flow on boiling from a tube in a bundle. Int. J. Heat Mass Transfer 33, 2579–2584.
Dhir, V.K., 1991. Nucleate and transition boiling heat transfer under pool and external flow conditions. Int. J. Heat Fluid Flow 12, 290–314.
Dhir, V.K., Liaw, S.P., 1989. Framework for a unified model for nucleate and transition pool boiling. ASME J. Heat Transfer 111, 739–746.
Flinta, J., Gernborg, G., Adesson, H., 1971. Results from the Blowdown Test for the Exercise. European Two-Phase Flow, Group Meeting, Denmark, June.
Gaertner, R.F., 1965. Photographic study of nucleate boiling on a horizontal surface. ASME J. Heat Transfer 87, 17–29.
Galloway, J.E., Mudawar, I., 1993. CHF mechanism in flow boiling from a short heated wall-II. Theoretical CHF model. Int. J. Heat Mass Transfer 36, 2527–2540.
Gaspari, G.P., Granzini, R., Hassid, A., 1973. Dryout onset in flow stoppage, depressurization and power surge transients. Energia Nucl. 20, 554.
Griffith, P., Pearson, J.F., Lepkowski, R.J., 1977. Critical heat flux during a loss-of-coolant accident. Nucl. Safety 18, 298–305.
Ha, S.J., No, H.C., 1998a. A dry-spot model of critical heat flux in pool and forced convection boiling. Int. J. Heat Mass Transfer 41, 303–311.
Ha, S.J., No, H.C., 1998b. A dry-spot model for transition boiling heat transfer in pool boiling. Int. J. Heat Mass Transfer 41, 3771–3779.
Ha, S.J., No, H.C., 2000. A dry-spot model of critical heat flux applicable to both pool boiling and subcooled forced convection boiling. Int. J. Heat Mass Transfer 43, 241–250.
Haider, S.I., Webb, R., 1997. A transient micro-convention model of nucleate pool boiling. Int. J. Heat Mass Transfer 40, 3675–3688.
Han, C.Y., Griffith, P., 1965. The mechanism of heat transfer in nucleate pool boiling. Int. J. Heat Mass Transfer 8, 887–914.
Haramura, Y., Katto, Y., 1983. A new hydrodynamic model of critical heat flux, applicable widely to both pool and forced convection boiling on submerged bodies in saturated liquids. Int. J. Heat Mass Transfer 26, 389–399.
Hassid, A., 1973. Critical heat flux (burnout) in transients: remarks on the available information. Energia Nucl. 20, 699–705.
Hein, D., Mayinger, F., 1972. Burnout power in transient conditions. European Seminar on Two-Phase Flow Thermohydraulics, Rome, June.
Hewitt, G.F., Govan, A.H., 1990. Phenomena and Prediction in Annular Two-Phase Flow. ASME Winter Annual Meeting, Dallas, pp. 41–56.
Hicken, E., Koch, E., Schad, O., 1972. Heat transfer during blowdown with an inside cooled tube as test section. CREST Specialist Mtg. On Emergency Core Cooling (ECC) for Light Water Reactors, Munich.
Hsieh, S.-S., Hsu, P.-T., 1994. Nucleate boiling characteristics of R-114, distilled water (H_2O) and R-134a on plain and rib-roughened tube geometries. Int. J. Heat Mass Transfer 37, 1423–1432.
Hsieh, S.-S., Ke, C.-G., 2002. Bubble dynamic parameters and pool boiling heat transfer on plasma coated tubes in saturated R-134a and R-600a. Trans. ASME J. Heat Transfer 124, 704–716.
Hsieh, S.-S., Yang, T.-Y., 2001. Nucleate pool boiling from coated and spirally wrapped tubes in saturated R-134a and R-600a at low and moderate heat flux. Trans. ASME J. Heat Transfer 123, 257–270.
Hsieh, S.-S., Huang, G.-Z., Tsai, H.-H., 2003a. Nucleate pool boiling characteristics from coated tube bundles in saturated R-134a. Int. J. Heat Mass Transfer 46, 1223–1239.
Hsieh, S.-S., Lai, W.-C., Tsai, H.-H., 2003b. LDV assisted bubble dynamic parameter measurements from two enhanced tubes boiling in saturated R-134a. Int. J. Heat Mass Transfer 46, 4911–4923.
Inoue, A., Ui, A., Yamazaki, Y., Matsusita, H., Lee, S.R., 2000. Studies on cooling of high heat flux surface in fusion reactor by impinging planar jet flow. Fusion Eng. Des., 781–787.
Ishii, M., Jones, O., 1976. Derivation and application of scaling criteria for two-phase flows, two-phase flows and heat transfer. In: Proceedings of the NATO Advanced Study Institute, Turkey, vol. 1, p. 163.
Ishii, M., Kataoka, I., 1983. Similarity Analysis and Scaling Criteria for LWR's Under Single-Phase and Two-Phase Natural Circulation. NUREG/CR-3267, Argonne National Laboratory.
Iwamura, T., Kuroyanagi, T., 1982. Burnout characteristics under flow reduction condition. J. Nucl. Sci. Technol., 438–448.
Iwamura, T., Watanabe, H., Murao, Y., 1994a. Critical heat flux experiments under steady-state and transient conditions and visualization of CHF phenomenon with neutron radiography. Nucl. Eng. Des. 149, 195–206.
Iwamura, T., Watanabe, H., Murao, Y., 1994b. Critical heat flux experiments under steady-state and transient conditions and visualization of CHF phenomenon with neutron radiography. Nucl. Eng. Des. 149, 195–206.
Judd, R.L., Hwang, K.S., 1976. A comprehensive model for nucleate pool boiling heat transfer including microlayer evaporation. Trans. ASME J. Heat Transfer 117, 623–629.
Kang, M.-G., 2000. Effect of surface roughness on pool boiling heat transfer. Int. J. Heat Mass Transfer 43, 4073–4085.
Kataoka, I., Serizawa, A., Sakurai, A., 1983. Transient boiling heat transfer under forced convection. Int. J. Heat Mass Transfer, 583–595.
Katto, Y., 1994. Critical heat flux. Int. J. Multiphase Flow 20, 53–90.
Kenning, D.B.R., 2004. Optical studies of boiling heat transfer: insights and limitations. Int. J. Heat Fluid Flow 25, 209–222.
Kirby, D.B., Westwater, J.W., 1965. Bubble and vapor behavior on a heated horizontal plate during pool boiling near burnout. Chem. Eng. Prog. Symp., Ser. 61 (57), 238–248.
Kocamustafaogullari, G., Ishii, M., 1986. Reduced Pressure and Fluid-to-Fluid Scaling Laws for Two-Phase Flow Loop. NUREG/CR-4584, Argonne National Laboratory.
Lawson, C.G., 1971. Heat transfer from electrically heated rods during a simulated LOCA. Chem. Eng. Prog. Symp. Ser. 19, 1–9.
Lay, J.H., Dhir, V.K., 1995. Shape of vapor stem during nucleate boiling of saturated liquids. Trans. ASME J. Heat Transfer 117, 394–401.
Lee, C.H., Lin, K.W., 1993. Experimental investigation of flow transient critical heat flux at light water reactor conditions. Int. Commun. Heat Mass Transfer 20, 477–488.
Lee, C.H., Mudawaar, I., 1988. A mechanistic critical heat flux model for subcooled flow boiling based on local flow conditions. Int. J. Multiphase Flow 14, 711.
Leung, J.C.M., Gallivan, K.A., Henry, R.E., 1981. Critical heat flux predictions during blowdown transients. Int. J. Multiphase Flow 7, 677–701.
Lienhard, J.H., 1988. Burnout on cylinders. ASME J. Heat Transfer 110, 1271–1286.
Lienhard, J.H., Dhir, V.K., 1973. Hydrodynamic prediction of peak pool-boiling heat fluxes from finite bodies. Trans. ASME J. Heat Transfer 95, 152–158.
Memory, S.B., Akcasayar, N., Eraydin, H., Marto, P.J., 1995a. Nucleate pool boiling of R-114 and R-114–oil mixtures from smooth and enhanced surfaces – II. Tube bundles. Int. J. Heat Mass Transfer 38, 1363–1376.
Memory, S.B., Sugiyama, D.C., Marto, P.J., 1995b. Nucleate pool boiling of R-114 and R-114–oil mixtures from smooth and enhanced surfaces – I. Single tubes. Int. J. Heat Mass Transfer 38, 1347–1361.
Moore, F.D., Mesler, R.B., 1961. The measurement of rapid surface temperature fluctuations during nucleate boiling of water. AIChE J. 7, 620–624.
Morgan, C.D., Roy, D.H., Hedrick, R.A., Stoudt, R.H., Zielke, L.A, Gellerstedt, J.S., 1972. Analytical and experimental investigation of heat transfer during simulated cold-leg blowdown accidents. CREST Specialist Meeting on Emergency Core Cooling for Light Water Reactors, Munich.
Moxon, D., Edwards, P.A., 1967. Dryout during flow and power transients. In: Proceedings of the European Two-Phase Flow Group Meeting, Winfrith, UK.
Nishikawa, K., Fujita, Y., Uchida, S., Ohta, H., 1984. Effect of surface configuration on nucleate boiling heat transfer. Int. J. Heat Mass Transfer 27, 1559–1571.

Nishio, S., Tanaka, H., 2002. Simplified model predicting contact-line-length density at critical heat flux based on direct observation of boiling structure. JSME Int. J., Ser. B 45, 72–78.
Nishio, S., Tanaka, H., 2004. Visualization of boiling structures in high heat-flux pool-boiling. Int. J. Heat Mass Transfer 47, 4559–4568.
Nishio, S., Gotoh, T., Nagai, N., 1998. Observations of boiling structures in high heat-flux boiling. Int. J. Heat Mass Transfer 41, 3191–3201.
Nuclear Studies and Safety Department (NSSD), Ontario Hydro, 1981. Bruce NGS "A": Assessment of Large-Break Loss-of-Coolant Accidents. Report No. 81038.
Palen, J.W., Yarden, A., Taborek, J., 1972. Characteristics of boiling outside large-scale horizontal multi-tube bundles. AIChE Symp. Ser. 68, 50–61.
Pasamechmetoglu, K.O., Chappidi, P.R., Unal, C., Nelson, R.A., 1993. Saturated pool nucleate boiling mechanisms at high heat fluxes. Int. J. Heat Mass Transfer 36, 3859–3868.
Pasamehmetoglu, K.O., Nelson, R.A., Gunnerson, F.S., 1990. Critical heat flux modeling in forced convection boiling during power transients. J. Heat Transfer, ASME 112, 1058–1062.
Pascual, C.C., Jeter, S.M., Abdel-Khalik, S.I., 2002. Visualization of boiling bubble dynamics using a flat uniformly heated transparent surface. Int. J. Heat Mass Transfer 45, 691–696.
Paul, D.D., Abdel-Khalik, S.I., 1983. A statistical analysis of saturated nucleate boiling along a heated wire. Int. J. Heat Mass Transfer 26, 509–519.
Pioro, I.L., Cheng, S.C., Vasic, A.Z., Felisari, R., 2000. Some problems for bundle CHF prediction based on CHF measurements in simple flow geometries. Nucl. Eng. Des. 201, 189–207.
Pioro, I.L., Rohsenow, W., Doerffer, S.S., 2004. Nucleate pool-boiling heat transfer. I: review of parametric effects of boiling surface. Int. J. Heat Mass Transfer 47, 5033–5044.
Ramaswamy, C., Joshi, Y., Nakayama, W., Johnson, W.B., 2002. High-speed visualization of boiling from enhanced structure. Int. J. Heat Mass Transfer 45, 4761–4771.
Rohsenow, W.M., 1982. Pool boiling. In: Hetsroni, G. (Ed.), Handbook of Multiphase Systems. Hemisphere, Washington, DC (Chapter 6.2).
Sadasivan, P., Unal, C., Nelson, R., 1995. Perspective: issues in CHF modeling – the need for new experiments. Trans. ASME J. Heat Transfer 117, 558–567.
Saidi, M.H., Ohadi, M., Souhar, M., 1999. Enhanced pool boiling of R-123 refrigerant on two selected tubes. Appl. Therm. Eng. 19, 885–895.
Shih, T.D., 1974. Measurements of Transient Critical Heat Flux by Fluid Modeling. Ph.D. Thesis, Nuclear Engineering, Iowa State University.
Smirnov, O.K., Pashkov, L.T., Zaitsev, V.N., 1973. Investigation of CHF with decrease in flow through a heated tube. Therm. Eng., 122.
Sugawara, S., Shiba, K. 1987. Full scale dryout test and analysis of the time to dryout during flow and power transients. In: Proceedings of the ASME-JSME Thermal Engineering Joint Conference, pp. 447–454.
Sun, K.-H., Lienhard, J.H., 1970. The peak boiling heat flux on horizontal cylinders. Int. J. Heat Mass Transfer 13, 1425–1439.
Tadreas, N.E., Kazimi, M.S., 1990. Nuclear Systems I Thermal Hydraulic Fundamentals. Hemisphere Publishing Corporation, New York, NY.
Takata, Y., Hidaka, S., Cao, J.M., Nakamura, T., Yamamoto, H., Masuda, M., Ito, T., 2005. Effect of surface wettability on boiling evaporation. Energy 30, 209–220.
Theofanous, T.G., Tu, J.P., Dinh, A.T., Dinh, T.N., 2002. The boiling crisis phenomenon, part I: nucleation and nucleate boiling heat transfer. Exp. Therm. Fluid Sci. 26, 775–792.
Tong, L.S., 1972. Boiling Crisis and Critical Heat Flux. USAEC Critical Review Series, Report TID-25887.
Tong, L.S., Hewitt, G.F., 1972. Overall Viewpoint of Flow Boiling CHF Mechanisms. ASME Paper 72-HT-54.
Tong, L.S., Weisman, J., 1996. Thermal Analysis of Pressurized Water Reactor, third ed. American Nuclear Society, La Grange Park, IL.
Tong, L.S., Bishop, H.E., Bishop, W.E., Casterline, J.E., Matzner, B. 1965. Transient DNB Test on CVTR Fuel Assembly. ASME Paper No. 65-WA/NE-3.
Unal, C., Daw, V., Nelson, R.A., 1992. Unifying the controlling mechanisms for the critical heat flux and quenching: the ability of liquid to contact the hot surface. Trans. ASME J. Heat Transfer 114, 972–982.
Van Ouwerkerk, H.J., 1972. Burnout in pool boiling the stability of boiling mechanisms. Int. J. Heat Mass Transfer 15, 25–34.
Weisman, J., 1995. A phenomenological explanation of the relationship between steady state and transient CHF at subcooled or low quality conditions. Nucl. Eng. Des. 158, 157–160.
Weisman, J., Pei, B.S., 1983. Prediction of critical heat flux in flow boiling at low qualities. Int. J. Heat Mass Transfer 26, 1463–1477.
Weisman, J., Ying, S.H., 1985. A theoretically based critical heat flux prediction for rod bundles at PWR conditions. Nucl. Eng. Des. 85, 239–250.
Yu, C.L., Mesler, R.B., 1977. Study of nucleate boiling near the peak heat flux through measurements of transient surface temperature. Int. J. Heat Mass Transfer 20, 827–840.
Zhao, Y.-H., Masuoka, T., Tsuruta, T., 2002a. Unified theoretical prediction of fully developed nucleate boiling and critical heat flux based on a dynamic microlayer model. Int. J. Heat Mass Transfer 45, 3189–3197.
Zhao, Y.-H., Masuoka, T., Tsuruta, T., 2002b. Theoretical studies on transient pool boiling based on microlayer model. Int. J. Heat Mass Transfer 45, 4325–4331.
Zielke, L.A., Wilson, R.H., 1974. Transient critical heat flux and spacer grid studies. Nucl. Technol. 24, 1.
Zuber, N., 1958. Stability of boiling heat transfer. ASME J. Heat Transfer 80, 711–720.